

PS.^{34–41} However, photocatalytic technology has been limited by low energy conversion rates,⁴² resulting in low or moderate yields of benzoic acid from PS degradation. Pure oxygen is usually required as an oxidant to further improve the oxidative efficiency (Scheme 1, method C). In addition, some other methods for degrading PS, including electrochemical degradation,⁴³ biodegradation,^{44,45} and ultrasonic degradation,⁴⁶ have also been developed recently (Scheme 1, method D). However, methods for degrading PS remain limited. Therefore, it is crucial and urgent to develop a green, clean and simple method for degrading PS to recover high-value chemical products.

Previously, we developed a catalytic system based on porphyrin-based porous organic polymers (PPOPs) and applied it to various dehydrogenation reactions.^{47,48} We found that these PPOPs can be very efficient at generating reactive oxygen species (ROS) in air. Porous organic polymers (POPs) are constructed by rigid monomers through irreversible covalent bonds, which endow them with high structural and chemical stability in various solvents and under harsh conditions.^{49,50} Porphyrins and their derivatives are a class of photosensitizers, which have a wide range of applications in photocatalytic reactions.^{47,48} Singlet oxygen (¹O₂) is a kind of ROS, which can induce the oxidation of various molecules. It is widely used in chemical reactions, biochemical processes and organic pollutant treatment.^{51–57} Xiao's group has demonstrated that ¹O₂ can efficiently seize a proton from the benzylic C–H bond of PS by hydrogen atom transfer (HAT), which produces benzyl radicals, further induces the oxidative degradation of PS, and finally obtains benzoic acid.³⁶ The critical role of ¹O₂ inspired us to consider whether the PPOPs can trigger the degradation of PS efficiently even in the air.

Herein, 7 different PPOPs by copolymerization of bromo-substituted porphyrins and diynes were afforded with different structures. Taking advantage of the porous structures and confined spaces, PPOPs could efficiently produce ROS under air and at room temperature compared to porphyrin monomers and achieve more efficient photocatalytic oxidative degradation of PS. Moreover, PPOPs have high structural and chemical stability. Impressively, controlled experiments have shown that PPOPs exhibit overwhelming advantages over those small-molecule photosensitizers. Therefore, such PPOPs provide an excellent photocatalytic platform for the oxidative degradation of PS (Scheme 1).

Initially, we synthesized the photocatalyst **PPOP-1** by the Sonogashira polycondensation according to a method reported in the literature.^{47,48} We performed a series of characterization methods for the obtained **PPOP-1** to confirm its structure (Fig. S1–S6, in the ESI†). Then we used PS (*M*_w ~ 350 000 g mol⁻¹) as a model substrate to optimize the oxidative degradation conditions. We surprisingly found that **PPOP-1** (5 mol%) can effectively catalyze the degradation of PS using *p*-toluenesulfonic acid monohydrate (*p*-TsOH·H₂O) (10 mol%) as an additive under the irradiation of black light (365–370 nm, 20 W) in ethyl acetate (EtOAc), yielding 48% of benzoic acid (Table 1, entry 1). Light and air were necessary for

Table 1 Optimization of the reaction conditions^{a,b}

| Entry | PPOP-1 (mol%) | Additive (mol%) | Solvent | Yield ^c (%) |
|-----------------|----------------------|--|--------------|------------------------|
| 1 | 5 | <i>p</i> -TsOH·H ₂ O (10) | EtOAc | 49 (48) |
| 2 | 5 | <i>p</i> -TsOH·H ₂ O (10) | DCE | 44 |
| 3 | 5 | <i>p</i> -TsOH·H ₂ O (10) | Acetone | 27 |
| 4 | 5 | <i>p</i> -TsOH·H ₂ O (10) | MeCN | Trace |
| 5 | 5 | <i>p</i> -TsOH·H ₂ O (10) | DMC | 45 |
| 6 | 2.5 | <i>p</i> -TsOH·H ₂ O (10) | EtOAc | 44 |
| 7 | 10 | <i>p</i> -TsOH·H ₂ O (10) | EtOAc | 50 |
| 8 | 5 | <i>p</i> -TsOH·H ₂ O (5) | EtOAc | 38 |
| 9 | 5 | <i>p</i> -TsOH·H ₂ O (20) | EtOAc | 50 |
| 10 | 5 | HCl (10) | EtOAc | 35 |
| 11 | 5 | CF ₃ COOH (10) | EtOAc | 26 |
| 12 | 5 | ZnCl ₂ (10) | EtOAc | 37 |
| 13 | 5 | Yb(OTf) ₃ (10) | EtOAc | 33 |
| 14 | 5 | Sc(OTf) ₃ (10) | EtOAc | 36 |
| 15 ^d | 5 | <i>p</i> -TsOH·H ₂ O (10) | EtOAc | 55 |
| 16 ^e | 5 | <i>p</i>-TsOH·H₂O (10) | EtOAc | 63 (62) |

^a The reaction was carried out with PS (0.2 mmol based on C₈H₈ as the repeating unit of PS, 1.0 equiv.) in the presence of 5 mol% **PPOP-1** and 10 mol% additive in 2 mL solvent under air, black light (365–370 nm, 20 W) and room temperature for 16 h. ^b The amounts of **PPOP-1**, additive and the yield of products were based on the repeating unit of PS. ^c Yield was determined by the crude ¹H NMR spectrum with 1,3,5-trimethoxybenzene as an internal standard; isolated yield in parentheses. ^d Room temperature for 32 h. ^e Room temperature for 48 h.

the degradation since PS could not be degraded without them (Table S1, entries 2 and 3 in the ESI†). Among different light sources, black light (365–370 nm, 20 W) performed best for acquiring benzoic acid (Table S1, entries 1 and 4–6 in the ESI†). In the case of using photosensitizers without additives, 26% yield of benzoic acid could be obtained (Table S1, entry 7 in the ESI†). Similarly, only 18% yield of benzoic acid could be obtained using additives without photosensitizers (Table S1, entry 8 in the ESI†), which corresponded to the literature reporting that acids could catalyze PS degradation to a certain extent.³⁶ Next, different solvents were screened (Table 1, entries 1–5). The results showed that the yield of benzoic acid using 1,2-dichloroethane (DCE) and dimethyl carbonate (DMC) as solvents was slightly lower than that using EtOAc, while no reaction occurred using other solvents. It might be due to the high solubility of PS in EtOAc.³⁷ Then, the amount of photosensitizer was studied and the results indicated that 5 mol% photosensitizer was the optimized loading equivalent (Table 1, entries 1, 6 and 7). The type and amount of additive was next optimized to be 10 mol% *p*-TsOH·H₂O, with the highest yield of benzoic acid (Table 1, entries 1, 8–14, see Table S1† for more details). As the reaction time was extended to 32 hours and 48 hours, the yield of benzoic acid was also gradually increased. Finally, 62% yield of benzoic acid was afforded in 48 hours (Table 1, entries 15 and 16). More optimization details for solvents, additives, amounts of photosensitizers and additives, and light sources are given in the ESI (Table S1†).

With the optimized reaction conditions in hand, several photocatalysts were evaluated systematically, including some commercially available small-molecule photosensitizers and different PPOPs (Table 2, entries 1–10; see Fig. 1, Fig. S9 and Table S2† for more details). Among these small-molecule photosensitizers, tetrabutylammonium decatungstate (TBADT) (Table 2, entry 1) and 9-mesityl-10-methylacridinium tetrafluoroborate (Mes-Acr-MeBF₄) (Table 2, entry 2) promoted such transformation slightly, while 1,2,3,5-tetrakis(carbazol-9-yl)-4,6-dicyanobenzene (4CzIPN) (Table S2, entry 3 in the ESI†), tris(2,2'-bipyridyl)ruthenium(II) dichloride hexahydrate (Ru(bpy)₃(Cl)₂·6H₂O) (Table S2, entry 4 in the ESI†) and bis[2-(2,4-difluorophenyl)-5-trifluoromethylpyridine][2-2'-bipyridyl] iridium hexafluorophosphate ([Ir(dF(CF₃)ppy)₂(dtbbpy)]PF₆) (Table S2, entry 5 in the ESI†) were not effective. The small-molecular porphyrin photosensitizers such as 5,10,15,20-tetraphenylporphyrin (TPP) (Table 2, entry 3) and 5,10,15,20-tetra(4-carboxyphenyl)-porphyrin (TCPP) (Table S2, entry 7 in the ESI†) exhibited a poor oxidative degradation effect on PS. Based on the structure of PPOP-1, we designed another six PPOPs by changing the structure of porphyrins and diynes and evaluated their photocatalytic effects (Table 2, entries 4–10). We were delighted to find that all the PPOPs containing porphyrin components showed much higher photodegradation efficiency of PS than small-molecule photosensitizers, among which PPOP-7 with a reduced tetraphenylporphyrin structure showed the optimal effect (71% yield of benzoic acid) (Fig. S11–S17 in the ESI†). This may be due to the large specific surface area (270.07 m² g⁻¹) and suitable pore size (2.6 nm) of PPOP-7. Therefore, in the following experiments, PPOP-7 was chosen as a photocatalyst for the degradation of PS-based plastic waste.

Subsequently, we applied PPOP-7 to the photodegradation of PS with different molecular weights and styrene copolymers

Table 2 Optimization of various photocatalysts^a

| Entry | Photocatalyst | Yield ^b (%) |
|-------|---------------------------|------------------------|
| 1 | TBADT | 25 |
| 2 | Mes-Acr-MeBF ₄ | 36 |
| 3 | TPP | 17 |
| 4 | PPOP-1 | 63 (62) |
| 5 | PPOP-2 | 61 |
| 6 | PPOP-3 | 60 |
| 7 | PPOP-4 | 62 |
| 8 | PPOP-5 | 61 |
| 9 | PPOP-6 | 65 |
| 10 | PPOP-7 | 71 (71) |

^a Reaction conditions: PS (0.2 mmol based on C₈H₈ as the repeating unit of PS, 1.0 equiv.), photocatalyst (0.01 mmol, 5 mol%), *p*-TsOH·H₂O (0.02 mmol, 10 mol%), EtOAc (2.0 mL), black light (365–370 nm, 20 W), open in air, and room temperature for 48 h.

^b Yield was determined by the crude ¹H NMR spectrum with 1,3,5-trimethoxybenzene as an internal standard; isolated yield in parentheses.

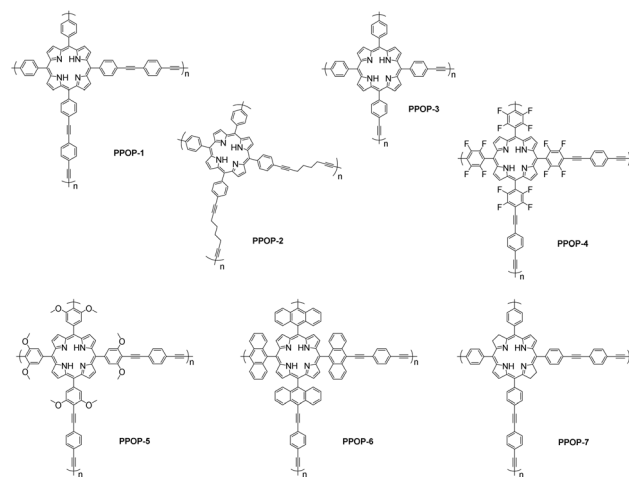


Fig. 1 Structures of photocatalysts, PPOPs.

with different structural units (Table 3). For the PS with different molecular weights, it could be well aerobically degraded to benzoic acid, and 69–72% yields could be obtained (Table 3, entries 1–4). For the copolymers of styrene, the yields of benzoic acid were not as high as those of PS. HIPS, graft-copolymerized by styrene and butadiene with strong impact strength, could be degraded to benzoic acid in 50% yield (Table 3, entry 5). Styrene-based block copolymers like SAN and ABS possess strong heat resistance and stability due to their acrylonitrile units, which makes their chemical degradation full of challenges.³⁹ Considering that the solubi-

Table 3 Aerobic degradation of polymers containing a styrene structural unit with different molecular weights^a

| Entry | Polymer | Yield (%) of benzoic acid ^b |
|----------------|---|--|
| 1 | PS-1 (<i>M_w</i> ~ 65 000 g mol ⁻¹) | 72 |
| 2 | PS-2 (<i>M_w</i> ~ 192 000 g mol ⁻¹) | 71 |
| 3 | PS-3 (<i>M_w</i> ~ 350 000 g mol ⁻¹) | 71 |
| 4 | PS-4 (<i>M_w</i> ~ 650 000 g mol ⁻¹) | 69 |
| 5 | HIPS (<i>M_w</i> ~ 140 000 g mol ⁻¹ , styrene 30 wt%) | 50 |
| 6 ^c | SAN (<i>M_w</i> ~ 165 000 g mol ⁻¹ , styrene 75 wt%) | 42 |
| 7 ^c | ABS (<i>M_w</i> ~ 238 000 g mol ⁻¹ , styrene 72 wt%) | 40 |

^a Reaction conditions: polymer (0.2 mmol based on C₈H₈ as the repeating unit of PS, 1.0 equiv.), PPOP-7 (0.01 mmol, 5 mol%), *p*-TsOH·H₂O (0.02 mmol, 10 mol%), EtOAc (2.0 mL), black light (365–370 nm, 20 W), open air, and room temperature for 48 h. ^b Isolated yield. ^c Acetone (2 mL) was used as the solvent and TFA (0.02 mol, 10 mol%) was used as the additive.

lity of SAN and ABS in acetone is much better than that in EtOAc, we used acetone as the solvent with trifluoroacetic acid (TFA) as the additive instead of *p*-TsOH·H₂O to give a desired yield of benzoic acid (40–42% yields) (Table 3, entries 6 and 7). In summary, polymers containing a styrene structural unit can be aerobically degraded efficiently to produce benzoic acid as the only product. The method we disclosed provides a convenient way for the degradation of such plastics under green and mild conditions.

According to the above experimental results, we finally investigated the aerobic degradation of waste PS products from daily life. As shown in Table 4, these waste PS products can be aerobically degraded to benzoic acid. PS wastes like these from EPS foams, plastic plates, food boxes, cup lids, yoghurt containers and packaging were all suitable as substrates, providing benzoic acid with 54–65% isolated yields (Table 4, entries 1–6). In addition, it is worth noting that for the degradation of SBS plastic, benzoic acid could also be obtained in a 44% isolated yield (Table 4, entry 7). These results demonstrated the practicality and potential applications of this polymer degradation strategy.

A series of tracking methods were used to reveal the degradation process. By sampling and analyzing the photodegradation process of PS, we could observe that the water contact angle on the PS membrane decreased with the progress of degradation, which indicated that the hydrophilicity of the membrane was enhanced, and a large number of hydrophilic groups, such as hydroxyl and carboxyl groups, were produced during the degradation process (Fig. 2a). An X-ray diffraction

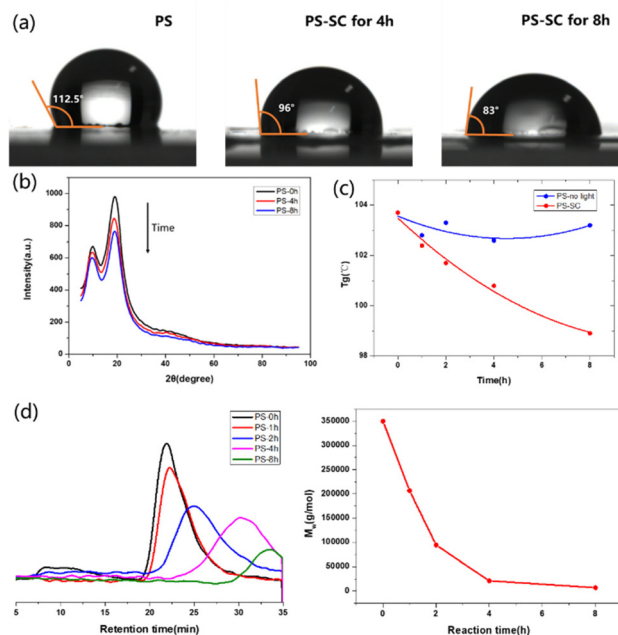


Fig. 2 Characterization of polymer degradation (SC: standard conditions). (a) Comparison of water contact angles on the top surface of PS-based membranes. (b) X-ray diffraction of PS depolymerization. (c) Tracing of glass transition temperature for PS degradation when reacting with or without light. (d) GPC tracing and the degradation trend for PS.

Table 4 Aerobic degradation of polymer waste from our daily life^a

| Entry | Substrate | Yield (%) ^b | Entry | Substrate | Yield (%) ^b |
|-------|---------------------------------|------------------------|-------|---------------------------------|------------------------|
| 1 | expanded polystyrene foam waste | 63 | 2 | polystyrene plastic plate waste | 65 |
| 3 | polystyrene food box waste | 54 | 4 | polystyrene cup lid waste | 58 |
| 5 | yogurt container waste | 55 | 6 | polystyrene packaging waste | 58 |
| 7 | SBS plastics | 44 | | | |

^a Reaction conditions: polymer waste (0.2 mmol based on C₈H₈ as the repeating unit of PS, 1.0 equiv.), PPOP-7 (0.01 mmol, 5 mol%), *p*-TsOH·H₂O (0.02 mmol, 10 mol%), EtOAc (2.0 mL), black light (365–370 nm, 20 W), open air, and room temperature for 48 h.
^b Isolated yield.

(XRD) experiment was further used to track the change of PS at different degradation times, which showed that the original crystal peak of PS gradually decreased upon degradation (Fig. 2b). The XRD experiment was also carried out using the PS degradation product (48 hours of degradation). From the obtained images, obvious diffraction peaks could be seen, indicating that benzoic acid was generated (Fig. S19b in the ESI†). The control experiments of PS in EtOAc with or without light were conducted, and the changes in glass transition temperature (*T_g*) with degradation time in these two cases were recorded. It could be clearly seen that PS was gradually decomposed during the reaction (Fig. 2c, red line, and Fig. S20 in the ESI†). The degradation process of PS under standard reaction conditions was monitored by gel permeation chromatography (GPC). Through the decrease of molecular weight, we could see that PS was gradually degraded during the reaction (Fig. 2d).

In order to elucidate the possible reaction pathways, a series of controlled experiments were carried out. Under standard conditions, the degradation experiments were conducted in the presence of 9,10-diphenylanthracene (DPA) or NaN₃ as an ¹O₂ trap or scavenger;³⁶ however, the expected degradation products were not obtained (Scheme 2, eqn (1)). These results suggested that ¹O₂ played crucial roles in the aerobic degradation of PS. In addition, a radical trap experiment was designed using 2,2,6,6-tetramethylpiperidin-1-oxyl (TEMPO) as the radical scavenger. No degradation of PS occurred under standard conditions with the addition of TEMPO, indicating



Scheme 2 Controlled experiments.

that the radical also contributed to the degradation of PS (Scheme 2, eqn (2)).

Based on the above experimental results and related literature reports,^{35–38,57} we proposed a possible reaction mechanism (Fig. 3). $^1\text{O}_2$ was first produced by two possible pathways. One way was that the electrophilic protonation of PS initially occurred under acidic reaction conditions to form an aromatic cation species **A**. Under the irradiation of black light, **A** was further excited to form an excited state **A***. The excited state **A*** underwent energy transfer with triplet oxygen ($^3\text{O}_2$), which led to the generation of $^1\text{O}_2$. Another way was that the photocatalyst **PPOP-7** was irradiated to an excited state **PPOP-7***, which could generate $^1\text{O}_2$ by energy transfer from $^3\text{O}_2$. The $^1\text{O}_2$ could react with **1** (PS) via the HAT process to produce benzyl radical **2** and $^{\cdot}\text{OOH}$. Next, $^{\cdot}\text{OOH}$ reacted with benzyl radical **2** to generate the corresponding peroxide intermediate **3**. Homolytic O–O bond cleavage under the irradiation of black light yielded the oxygen radical **4** and the hydroxyl radical ($^{\cdot}\text{OH}$). **4** underwent a β -scission to produce fragments **5** and **6**, which with repeated HAT and β -scission processes generated benzoylformic acid **7**. Under light irradiation, **7** underwent decarbonylation to form benzoyl radical **8** with CO and $^{\cdot}\text{OH}$ removal. Benzaldehyde **9** was formed from benzoyl radical **8** by HAT, which was further oxidized to afford benzoic acid **10**.

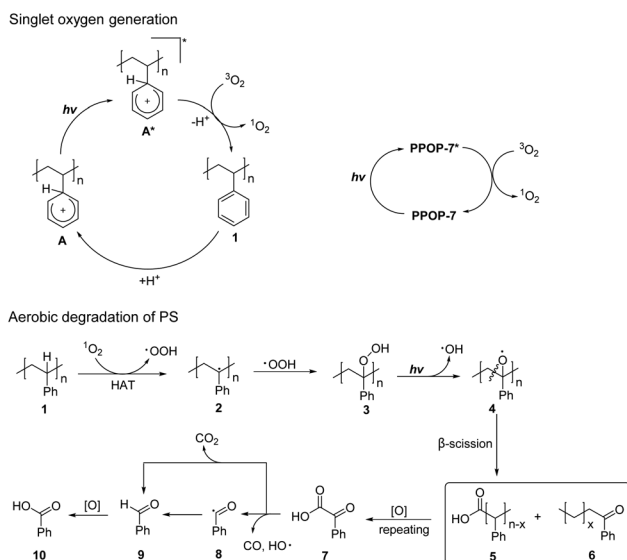


Fig. 3 Proposed reaction mechanism.

Alternatively, **7** underwent a decarboxylation process to directly obtain benzaldehyde **9** with CO_2 release, which was then oxidized to obtain benzoic acid **10**.

Conclusions

In summary, the efficient and green degradation of polystyrene under air was realized using a porphyrin-based porous organic polymer (PPOP) as a photocatalyst. Benzoic acid was obtained as the only product with good selectivity and yield (up to 72% yield). This approach for the degradation of plastics features mild conditions, green solvents, simple operation, and air as the oxidant. It can convert a wide range of polystyrene wastes into high-value products by upcycling. This method is also suitable for other polymers containing a styrene structural unit to obtain benzoic acid. Mechanistic studies have demonstrated that both $^1\text{O}_2$ and radicals play crucial roles in the degradation process. We believe that this photo-induced oxidative degradation will not only provide a unique method for upcycling real plastic wastes, but also address the increasingly serious environmental crisis in the future.

Author contributions

N. Z. designed the study. S. X. and S. L. performed the experiments and analyzed the data. S. X., S. L., W. S. and N. Z. wrote the manuscript.

Conflicts of interest

The authors declare no competing interests.

Acknowledgements

This work was supported by grants from the National Natural Science Foundation of China (22375027), the Natural Science Foundation of Jiangsu Province (BK20221265 and BK20211100), and the Fundamental Research Funds for the Central Universities (DUT23YG133). The authors acknowledge the assistance of the Dalian University of Technology (DUT) Instrumental Analysis Center.

References

- 1 N. Simon, K. Raubenheimer, N. Urho, S. Unger, D. Azoulay, T. Farrelly, J. Sousa, H. van Asselt, G. Carlini, C. Sekomo, M. L. Schulte, P.-O. Busch, N. Wienrich and L. Weiland, *Science*, 2021, **373**, 43–47.
- 2 R. Geyer, J. R. Jambeck and K. L. Law, *Sci. Adv.*, 2017, **3**, e1700782.
- 3 A. Rahimi and J. M. García, *Nat. Rev. Chem.*, 2017, **1**, 0046.

- 4 R. Meys, A. Kätelhön, M. Bachmann, B. Winter, C. Zibunas, S. Suh and A. Bardow, *Science*, 2021, **374**, 71–76.
- 5 S. S. Borkar, R. Helmer, F. Mahnaz, W. Majzoub, W. Mahmoud, M. Al-Rawashdeh and M. Shetty, *Chem Catal.*, 2022, **2**, 3320–3356.
- 6 A.-C. Albertsson and M. Hakkarainen, *Science*, 2017, **358**, 872–873.
- 7 L. E. Revell, P. Kuma, E. C. Le Ru, W. R. C. Somerville and S. Gaw, *Nature*, 2021, **598**, 462–467.
- 8 A. Stubbins, K. L. Law, S. E. Muñoz, T. S. Bianchi and L. Zhu, *Science*, 2021, **373**, 51–55.
- 9 R. G. Santos, G. E. Machovsky-Capuska and R. Andrades, *Science*, 2021, **373**, 56–60.
- 10 M. MacLeod, H. P. H. Arp, M. B. Tekman and A. Jahnke, *Science*, 2021, **373**, 61–65.
- 11 L. Weiss, W. Ludwig, S. Heussner, M. Canals, J.-F. Ghiglione, C. Estournel, M. Constant and P. Kerhervé, *Science*, 2021, **373**, 107–111.
- 12 S. B. Borrelle, J. Ringma, K. L. Law, C. C. Monnahan, L. Lebreton, A. McGivern, E. Murphy, J. Jambeck, G. H. Leonard, M. A. Hilleary, M. Eriksen, H. P. Possingham, H. De Frond, L. R. Gerber, B. Polidoro, A. Tahir, M. Bernard, N. Mallos, M. Barnes and C. M. Rochman, *Science*, 2020, **369**, 1515–1518.
- 13 A. Milbrandt, K. Coney, A. Badgett and G. T. Beckham, *Resour., Conserv. Recycl.*, 2022, **183**, 106363.
- 14 K. Ragaert, L. Delva and K. Van Geem, *Waste Manage.*, 2017, **69**, 24–58.
- 15 G. W. Coates and Y. D. Y. L. Getzler, *Nat. Rev. Mater.*, 2020, **5**, 501–516.
- 16 I. Vollmer, M. J. F. Jenks, M. C. P. Roelands, R. J. White, T. van Harmelen, P. de Wild, G. P. van der Laan, F. Meirer, J. T. F. Keurentjes and B. M. Weckhuysen, *Angew. Chem., Int. Ed.*, 2020, **59**, 15402–15423.
- 17 L. D. Ellis, N. A. Rorrer, K. P. Sullivan, M. Otto, J. E. McGeehan, Y. Román-Leshkov, N. Wierckx and G. T. Beckham, *Nat. Catal.*, 2021, **4**, 539–556.
- 18 L. T. J. Korley, T. H. Epps, B. A. Helms and A. J. Ryan, *Science*, 2021, **373**, 66–69.
- 19 C. Jehanno, J. W. Alty, M. Roosen, S. De Meester, A. P. Dove, E. Y. X. Chen, F. A. Leibfarth and H. Sardon, *Nature*, 2022, **603**, 803–814.
- 20 J. Nisar, G. Ali, A. Shah, M. R. Shah, M. Iqbal, M. N. Ashiq and H. N. Bhatti, *Energy Fuels*, 2019, **33**, 12666–12678.
- 21 J. Wang, J. Jiang, X. Wang, R. Wang, K. Wang, S. Pang, Z. Zhong, Y. Sun, R. Ruan and A. J. Ragauskas, *J. Hazard. Mater.*, 2020, **386**, 121970.
- 22 O. Dogu, A. Eschenbacher, R. John Varghese, M. Dobbelaere, D. R. D'Hooge, P. H. M. Van Steenberge and K. M. Van Geem, *Chem. Eng. J.*, 2023, **455**, 140708.
- 23 S. Fan, Y. Zhang, L. Cui, T. Maqsood and S. Nižetić, *J. Cleaner Prod.*, 2023, **390**, 136102.
- 24 R. Li, Z. Zhang, X. Liang, J. Shen, J. Wang, W. Sun, D. Wang, J. Jiang and Y. Li, *J. Am. Chem. Soc.*, 2023, **145**, 16218–16227.
- 25 Z. Xu, F. Pan, M. Sun, J. Xu, N. E. Munyaneza, Z. L. Croft, G. G. Cai and G. Liu, *Proc. Natl. Acad. Sci. U. S. A.*, 2022, **119**, e2203346119.
- 26 N. E. Munyaneza, C. Posada, Z. Xu, V. De Altin Popiolek, G. Paddock, C. McKee and G. Liu, *Angew. Chem., Int. Ed.*, 2023, **62**, e202307042.
- 27 A. Pifer and A. Sen, *Angew. Chem., Int. Ed.*, 1998, **37**, 3306–3308.
- 28 K. P. Sullivan, A. Z. Werner, K. J. Ramirez, L. D. Ellis, J. R. Bussard, B. A. Black, D. G. Brandner, F. Bratti, B. L. Buss, X. Dong, S. J. Haugen, M. A. Ingraham, M. O. Konev, W. E. Michener, J. Miscall, I. Pardo, S. P. Woodworth, A. M. Guss, Y. Roman-Leshkov, S. S. Stahl and G. T. Beckham, *Science*, 2022, **378**, 207–211.
- 29 H. Huang, K. A. Steiniger and T. H. Lambert, *J. Am. Chem. Soc.*, 2022, **144**, 12567–12583.
- 30 X. Fang, Y. Tang, Y. Ma, G. Xiao, P. Li and D. Yan, *Sci. China Mater.*, 2023, **66**, 664–671.
- 31 X. Fang, R. Gao, Y. Yang and D. Yan, *iScience*, 2019, **16**, 22–30.
- 32 P. Li, T. Zhang, M. A. Mushtaq, S. Wu, X. Xiang and D. Yan, *Chem. Rec.*, 2021, **21**, 841–857.
- 33 P. Li, Y. Liu, M. A. Mushtaq and D. Yan, *Inorg. Chem. Front.*, 2023, **10**, 4650–4667.
- 34 G. Zhang, Z. Zhang and R. Zeng, *Chin. J. Chem.*, 2021, **39**, 3225–3230.
- 35 T. Li, A. Vijeta, C. Casadevall, A. S. Gentleman, T. Euser and E. Reisner, *ACS Catal.*, 2022, **12**, 8155–8163.
- 36 Z. Huang, M. Shanmugam, Z. Liu, A. Brookfield, E. L. Bennett, R. Guan, D. E. Vega Herrera, J. A. Lopez-Sanchez, A. G. Slater, E. J. L. McInnes, X. Qi and J. Xiao, *J. Am. Chem. Soc.*, 2022, **144**, 6532–6542.
- 37 Y. Qin, T. Zhang, H. Y. V. Ching, G. S. Raman and S. Das, *Chem*, 2022, **8**, 2472–2484.
- 38 S. Oh and E. E. Stache, *J. Am. Chem. Soc.*, 2022, **144**, 5745–5749.
- 39 J. Meng, Y. Zhou, D. Li and X. Jiang, *Sci. Bull.*, 2023, **68**, 1522–1530.
- 40 C. Li, X. Y. Kong, M. Lyu, X. T. Tay, M. Đokić, K. F. Chin, C. T. Yang, E. K. X. Lee, J. Zhang, C. Y. Tham, W. X. Chan, W. J. Lee, T. T. Lim, A. Goto, M. B. Sullivan and H. S. Soo, *Chem*, 2023, **9**, 2683–2700.
- 41 A. Ong, J. Y. Q. Teo, Z. Feng, T. T. Y. Tan and J. Y. C. Lim, *ACS Sustainable Chem. Eng.*, 2023, **11**, 12514–12522.
- 42 W. S. Koe, J. W. Lee, W. C. Chong, Y. L. Pang and L. C. Sim, *Environ. Sci. Pollut. Res.*, 2020, **27**, 2522–2565.
- 43 J. Lu, R. Hou, Y. Wang, L. Zhou and Y. Yuan, *Water Res.*, 2022, **226**, 119277.
- 44 P. Xiang, Y. Zhang, T. Zhang, Q. Wu, C. Zhao and Q. Li, *J. Hazard. Mater.*, 2023, **458**, 131856.
- 45 Z. Chen, Y. Zhang, R. Xing, C. Rensing, J. Lü, M. Chen, S. Zhong and S. Zhou, *Environ. Sci. Technol.*, 2023, **57**, 7867–7874.

- 46 J. Zimmermann, D. Kruppa, M. Fischlschweiger, S. Beuermann and S. Enders, *Chem. Ing. Tech.*, 2021, **93**, 289–296.
- 47 X. Sun, N. Zheng, G. Liu, Q. Wu and W. Song, *Chem. Commun.*, 2022, **58**, 13234–13237.
- 48 J. Bai, X. Xu, Y. Zheng, W. Song and N. Zheng, *Green Synth. Catal.*, 2023, DOI: [10.1016/j.gresc.2023.03.001](https://doi.org/10.1016/j.gresc.2023.03.001).
- 49 Y. Zhang and S. N. Riduan, *Chem. Soc. Rev.*, 2012, **41**, 2083–2094.
- 50 S. B. Yu, F. Lin, J. Tian, J. Yu, D. W. Zhang and Z. T. Li, *Chem. Soc. Rev.*, 2022, **51**, 434–449.
- 51 A. Sagadevan, K. C. Hwang and M.-D. Su, *Nat. Commun.*, 2017, **8**, 1812.
- 52 S. Ren, H. Li, X. Xu, H. Zhao, W. He, L. Zhang and Z. Cheng, *Biomater. Sci.*, 2023, **11**, 509–517.
- 53 M. Wang, J. Guo, L. Chen and X. Zhao, *Biomater. Sci.*, 2023, **11**, 1776–1784.
- 54 W. Wang, Y. Song, Y. Tian, B. Chen, Y. Liang, Y. Liang, C. Li and Y. Li, *Biomater. Sci.*, 2023, **11**, 2828–2844.
- 55 M. Wang, Y. Zheng, H. He, T. Lv, X. Xu, X. Fang, C. Lu and H. Yang, *Biomater. Sci.*, 2023, **11**, 7423–7431.
- 56 J. Al-Nu'airat, I. Oluwoye, N. Zeinali, M. Altarawneh and B. Z. Dlugogorski, *Chem. Rec.*, 2021, **21**, 315–342.
- 57 J. Wu, J. Chen, L. Wang, H. Zhu, R. Liu, G. Song, C. Feng and Y. Li, *Green Chem.*, 2023, **25**, 940–945.